

ADSORPTION OF BASIC MAGENTA USING FRESH WATER ALGAE AND BROWN MARINE SEAWEED: CHARACTERIZATION STUDIES AND ERROR ANALYSIS

S. DEVI*, A. MURUGAPPAN

Department of Civil Engineering, Annamalai University, Annamalainagar, 608002, India

*Corresponding Author: degisvinicivil2002@yahoo.co.in

Abstract

The batch studies were performed for sorption of Basic Violet 14 onto brown seaweed (*Gracilaria edulis*) and fresh water algae (*Lyngbya wollei*) to explore potential of sorbents. The effects of pH, sorbent dosage, temperature, shaking speed, contact time and particle size on the decolorization were investigated to establish optimal conditions. The uptake rate was rapid and attains equilibrium within 90 min. The experimental isotherm data were analyzed with Langmuir, Freundlich, Dubinin-Radushkevich, Temkin equations and well explained by Temkin model. The error functions, Sum of the Squares of the Errors, Hybrid Fractional Error Function, Marquardt's Percent Standard Deviation, Average Relative Error and Sum of Absolute Errors functions were used to determine the suitability of isotherm model with the sorption of Basic Violet 14. Both sorbents pursue Dubinin-Radushkevich isotherm model that is chemisorption, which has been confirmed with pseudo-second order and Elovich model. Fourier Transform Infrared spectra and Scanning electron microscopy images confirm the sorptivity of adsorbents. The pseudo-first-order, pseudo-second-order, initial sorption and intraparticle diffusion rate constants for different initial concentrations were deliberated for dye concentration of 20 to 100 mg/L. The diffusion rate of the dye molecules increases with increased dye concentration.

Keywords: Basic Violet 14, Fuch sine, Kinetics, Seaweed, Error analysis.

1. Introduction

Dyes are the main source of colour in effluents. Some industries that discharge highly coloured effluents are paper and pulp mills, textiles and dye-making industries, alcohol distilleries and leather industries. Moreover, these dyes may cause suspected carcinogenic and genotoxic effects [1]. Especially, basic dyes have

Nomenclatures

A_T	Temkin isotherm related to equilibrium binding constant, L/g
a	Elovich rate equation constants representing the initial rate of sorption, $mg/g/min$
B_T	Temkin isotherm constant
b	The extent of surface coverage and the activation energy of chemisorptions, g/mg
C_e	The equilibrium (residual) concentration of adsorbate in solution, mg/L
C_i	Initial dye concentration, mg/L
C_o	Dye concentration at any time, mg/L
I_1	The intercept of first stage adsorption
I_2	The intercept of second stage adsorption
K_{ad}	Dubinin–Radushkevich isotherm constant, mol^2/kJ^2
K_F	Freundlich isotherm constant, mg/g
K_L	Langmuir isotherm constant, L/mg
k_{id1}	The intraparticle diffusion rate constant of the first stage of adsorption, $mg/g-min^{0.5}$
k_{id2}	The intraparticle diffusion rate constant of the second stage of adsorption, $mg/g-min^{0.5}$
k_1	The equilibrium rate constant of pseudo-first sorption, min^{-1}
k_2	The equilibrium rate constant of pseudo-second order sorption, $g/mg/min$
m	Mass of the dry sorbent used, g
n	Adsorption intensity
q_e	The amount of dye adsorbed per gram of the adsorbent at equilibrium, mg/g
q_{max}	The maximum monolayer coverage capacity, mg/g
q_s	The theoretical isotherm saturation capacity, mg/g
q_t	The amount of dye adsorbed at time ' t ', mg/g
R	Universal gas constant, $8.314 J/mol/K$
T	Temperature, K
t	Sorption contact time, min
V	Volume of the solution, L

high brilliance and intensity of colours and are highly visible even in a very low concentration [2]. Thus, different techniques like coagulation, precipitation, biodegradation, oxidation, membrane separation, ion exchange and photo degradation have been employed to remove dyes from textile wastewater. These chemical or physical-chemical methods are less efficient, costly, of limited applicability and produce wastes, which are difficult to dispose of [3]. Among the available treatment technologies, adsorption is superior and reliable in simplicity of design, convenience, initial cost, ease of operation and insensitivity to the toxic substance [4, 5].

A large number of suitable adsorbents such as activated carbon, polymeric resins or various low cost adsorbents (non-modified or modified cellulose biomass, chitin, bacterial biomass, etc.) have been studied. The use of bio-

sorbents for removing various pollutants from water and wastewater offers many attractive features such as the outstanding adsorption capacity for many pollutants and the fact that these materials are low-cost, non-toxic and biocompatible [6]. Mutually, the studies are inadequate on improving the sorption capacities of adsorbents after chemical or appropriate treatment, eco-friendly disposal of spent sorbents [4]. Hence the limited literature should be enriched to enhance the use of bio-sorbents in industrial applications. Nonetheless, the attraction towards the use of bio-sorbents is merits over the various adsorbents as cheaper, renewable, locally and abundantly available [7].

In the current investigation, brown seaweed (*Gracilaria edulis*) and algae (*Lyngbya wollei*) were used to remove the dye Basic Violet 14 (BV 14) by adsorption from aqueous solution. The influence of some parameters such as solution pH, contact time, initial dye concentration, agitation speed, particle size, adsorbent dosage and temperature were studied. Kinetics and isotherm studies were also carried out to evaluate the adsorption capacity of both adsorbents.

2. Materials and methods

2.1. Dyestuff and aqueous solution

The Basic Magenta (Basic Violet 14) used was the commercial salt, which were widely used in textile industry. The Basic violet 14 (C.I. 42510) was purchased from HiMedia Private Ltd, India, with analytical grade and was further used without any purification. The stock dye solution was prepared by using deionised water to achieve concentration of 1000 mg/L. The requisite concentrations were obtained by diluting the stock solution of BV 14. Fresh dilutions were used for each experiment. The pH (3 to 10.5) of the working solutions was adjusted using 0.1N sodium hydroxide or hydrochloric acid solutions. The molecular weight of the dye is 337.85.

2.2. Sorbent

The *Lyngbya wollei* was collected from Veeranam Lake, Cuddalore District, Tamilnadu. The seaweed *Gracilaria edulis* was collected from mandabam, Rameshwaram, Tamilnadu. Then they were separately washed several times with tap water and then deionised water to remove dirt and small aquatic organisms. Afterwards, they were dried at room temperature for 24 hours. The algal samples were ground and sieved to different particle sizes and subsequently used for sorption experiments.

2.3. Sorption experiment

Batch experiments were performed to investigate the sorption of basic dye on sorbents. Exactly 100 ml of dye solution of known initial concentration (50 mg/L) was shaken at the certain agitation speed (25, 50, 100, 150, 200 rpm) with a required dose of adsorbents (1 to 5 g/L) for 90 min in an orbital shaker, with a range of pH (3 to 10.5) at various temperature (30, 35, 40, 45 and 50 °C). The final concentration (C_e) was measured. The concentration in the test solution was

determined using a UV Double beam spectrophotometer, (HITACHI U-2001) at a wavelength ($\lambda_{\max} = 549$ nm) corresponding to the maximum absorbance. The percentage removal of dye and adsorption capacity q_t (mg/g) at any time was calculated using the following equations [7]:

$$\text{Removal efficiency (\%)} = \frac{C_i - C_o}{C_i} * 100 \quad (1)$$

$$q_t = (C_i - C_o) * \left(\frac{V}{m}\right) \quad (2)$$

2.4. Isotherm studies

Isotherm states the relationship between adsorbate to adsorbent at constant temperature. Langmuir, Freundlich, Dubinin- Radushkevich and Temkin adsorption isotherms were employed to analyze the experimental data of sorption of BV 14 onto *L.wollei* and *G.edulis*.

The linear form of isotherms is represented as

Langmuir adsorption isotherm [8]:

$$\frac{1}{q_e} = \frac{1}{q_{\max}} + \frac{1}{k_L q_{\max} C_e} \quad (3)$$

Freundlich isotherm [9]:

$$\log q_e = \log K_F + \frac{1}{n} \log C_e \quad (4)$$

Dubinin – Radushkevich (D-R) isotherm model [10]:

$$\ln(q_e) = \ln(q_s) - k_{ad} \varepsilon^2 \quad (5)$$

where, Polanyi potential (ε) is given as

$$\varepsilon^2 = RT \ln \left(1 + \frac{1}{C_e}\right) \quad (6)$$

Temkin isotherm [11]:

$$q_e = \frac{RT}{B_t} \ln A_t + \left(\frac{RT}{B_t}\right) \ln C_e \quad (7)$$

2.5. Error functions

Five different error functions [12] were used to find out the most suitable isotherm model to signify the experimental data.

The Sum of the Squares of the Errors (ERRSQ /SSE): This is the most commonly used error function. It can be represented as

$$\sum_{i=1}^n (q_{e,cal} - q_{e,exp})_i^2 \tag{8}$$

Hybrid Fractional Error Function (HYBRID): It is used to improve the fit of the sum of the squares of the errors at low concentrations by dividing it by the measured value. It also includes the number of degrees of freedom of the system- the number of data points, n, minus the number of parameters, p, of the isotherm equation-as a divisor.

$$\frac{100}{n-p} \sum_{i=1}^n \left[\frac{q_{e,exp} - q_{e,cal}}{q_{e,exp}} \right]_i \tag{9}$$

Marquardt’s Percent Standard Deviation (MPSD): The MPSD is similar in some respects to a geometric mean error distribution modified according to the number of degrees of freedom of the system.

$$100 \sqrt{\frac{1}{n-p} \sum_{i=1}^n \left[\frac{q_{e,exp} - q_{e,cal}}{q_{e,exp}} \right]_i^2} \tag{10}$$

Average Relative Error (ARE): This error function attempts to minimise the fractional error distribution across the entire concentration range.

$$\frac{100}{n} \sum_{i=1}^n \left| \frac{q_{e,exp} - q_{e,cal}}{q_{e,exp}} \right|_i \tag{11}$$

Sum of Absolute Errors (EABS/SAE): This approach is similar to the sum of the squares of the errors. Isotherm parameters determined using this error function would provide a better fit as the magnitude of the error increased biasing the fit towards the high concentration data.

$$\sum_{i=1}^n |q_{e,exp} - q_{e,cal}|_i \tag{12}$$

2.6. Sorption kinetics

In this study, pseudo first order, pseudo second-order rate equation, Intra particle diffusion model and Elovich model were used to find the potential rate-controlling steps involved in the process of adsorption of BV 14 onto *L.wollei* and *G.edulis*.

The linear form of kinetic models is represented as

The pseudo-first order equation [13]:

$$\log(q_e - q_t) = \log(q_e) - \left(\frac{k_1}{2.303} \right) t \tag{13}$$

The pseudo-second order equation [14]:

$$\frac{t}{q_t} = \frac{1}{kq_e^2} + \frac{1}{q_e t} \tag{14}$$

The intra-particle diffusion model [15]:

$$q_t = K_{id} t^{0.5} + I \quad (15)$$

Elovich model [16, 17]:

$$qt = \left(\frac{1}{b}\right) \ln(ab) + \left(\frac{1}{b}\right) \ln t \quad (16)$$

2.7. Sorbent characterization

Scanning electron microscopy (SEM) images illustrate the surface morphology and fundamental physical properties of the adsorbent. Sorbents were characterized by scanning electron microscopy (SEM, Jeol JSM 5610, Japan). Powder sample was sprayed on the surface of the specimen stub using the double sided adhesive carbon tape and then samples were deposited with a thin layer of gold with the help of gold coater JEOL auto fine coater model JFS-1600.

The Fourier Transform Infrared (FTIR) spectra of the samples were recorded on Perkin Elmer FTIR spectrophotometer (Spectrum BX-II) using a pellet (pressed-disk) technique. One mg of adsorbent was intimately mixed with approximately 100mg of dry, powdered KBr.

3. Results and Discussion

3.1. Effect of parameters

The maximum dye uptake of BV 14 for various pH onto *L.wollei* and *G.edulis* biomass was studied while the initial dye concentration, shaking time, amount of sorbent, and temperature were fixed at 50 mg/L, 90 min, 0.20 g/100 ml, and 30°C, respectively. The dye adsorption was found to increase with an increase in pH from 3 to 6 and then decreased at pH 7; again it began to increase with pH 8 to 10. The lower dye uptake was recorded at pH 3. Lower dye uptake at acidic pH is probably due to the presence of excess H⁺ ions competing with the cation groups on the dye for adsorption sites. A small decrease in adsorption was observed when pH increased after pH 6 (exactly at pH 7). The decrease in uptake may be due to the formation of the zwitterion form of dye which makes the molecule bigger and unable to enter into the pores on the surface [18]. After pH 7, again the sorption was increased with increase in pH. Maximum uptake was at pH 10 in both cases (Fig. 1). At higher pH, the surface of sorbent particles may get negatively charged, which enhances the positively charged dye cations through electrostatic forces of attraction. A similar result of pH effect was reported for the adsorption of Rhodamine B onto carbon derived from scrap tires [19].

The effect of *L.wollei* and *G.edulis* biomass dosage on the amount of dye adsorbed was studied by varying the amount of sorbent from 1 to 5 g/L whereas the dye concentration of 50 mg/L. All these studies were conducted at room temperature and at a constant agitation speed of 150 rpm. Figure 2 shows the effect of adsorbent dosage on the amount of dye adsorbed and it was observed that the amount of dye adsorbed decreased and the percentage dye removal was increased with increase in sorbent dosage of 1 g/L to 5 g/L. This was because of the increased total surface area and availability of more sites [20]. The dye uptake decreased from 48.02 mg/g to 9.89 mg/g (*L.wollei*) and 48.06 mg/g to 9.8 mg/g

(*G.edulis*). An increase in dye uptake was observed to decrease in adsorbent dosage. This may be due to the decrease in the total adsorption surface area available to dye from overlapping or aggregation of adsorption sites [21]. A similar result of the sorbent dose effect was also reported for the removal of basic yellow 87 from aqueous solution by using two mesoporous materials: MCM41 and carbon aerogel (MCA) as adsorbents [22].

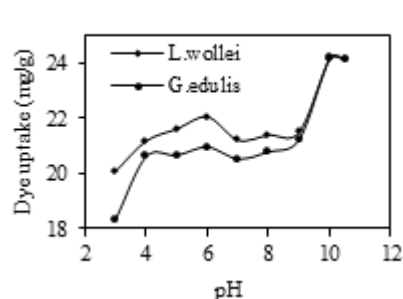


Fig. 1. Effect of pH on sorption of BV 14 by *L.wollei* and *G.edulis* biomass. Contact time- 90 min, initial dye concentration- 50 mg/L, sorbent dose- 0.2 g, agitation speed- 150 rpm, Room temperature

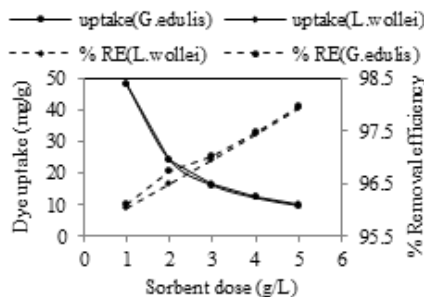


Fig. 2. Effect of sorbent dose on sorption of BV 14 by *L.wollei* and *G.edulis* biomass. Contact time - 90 min, pH- 10, initial dye concentration- 50 mg/L, agitation speed-150 rpm, Room temperature

The rate of BV 14 sorption onto *L.wollei* and *G.edulis* biomass was studied with a temperature range of 30, 35, 40, 45 and 50°C. Figure 3 shows the temperature profile revealing that the fitted adsorption capacity at equilibrium (q_e) increased, to some extent, with increasing temperature, i.e., 30°C to 40°C. The maximum sorption capacity was attained at 40°C for both sorbents. The fact that the rate of dye uptake is favoured by temperature indicates that the mobility of the dye molecules increases with a rise in the temperature [23]. Furthermore, the values of q_e decreased with increasing temperature i.e., 40°C to 50°C. This is for the reason that the biosorbent loses its properties at very high temperatures due to denaturation. The similar phenomena were observed by adsorption of ethyl violet dye in aqueous solution by regenerated spent bleaching earth [24].

Shaking consumes energy and affects the adsorption efficiency, so it is important to determine the optimal speed that should be used in wastewater treatment [25]. The dye sorption capacity of both fresh water algae and seaweed was studied for different shaking speed (25, 50, 100, 150, 200 rpm) at 40°C. The influence of agitation speed on adsorption of dye is shown in Fig. 4. The amount adsorbed at equilibrium (mg/g) was found to increase initially with increased in agitation speed from 25 to 50 rpm. This is due to the change in boundary layer resistance of the system. The maximum uptake of BV 14, 49.08 mg/g and 49.18 mg/g was obtained at 50 rpm by *L.wollei* and *G.edulis* respectively. But, the dye uptake then decreased at 100 rpm. This decrease in uptake capacity may be attributed to an increase desorption tendency of dye molecules and/or having a similar speed of adsorbent particles and adsorbate ions (i.e. the formation of a more stable film around the adsorbent particles).

This desorption tendency may be attributed to high mixing speed which means additional energy input and higher shear force causing break of newly formed bonds between dye and the adsorbent [26]. The dye uptake was again increased from 100 to 150 rpm which indicates that there is a chance of increase in boundary layer thickness still efficient due to deformation of stable film [27]. Though the shaking speed rose above 150 rpm, diffusion speeds decreased yet again. This is may be due to desorption tendency at higher mixing speed. The difference of adsorption rate at different agitation speed was insignificant. Thus, the optimum agitation speed was selected as 50 rpm.

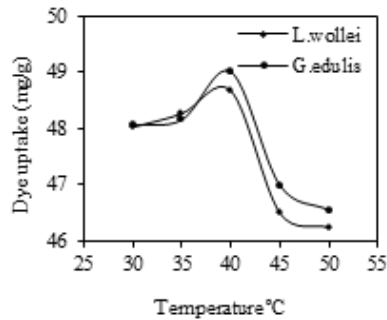


Fig. 3. Effect of temperature on sorption of BV 14 by *L.wollei* and *G.edulis* biomass. Contact time- 90 min, pH- 10, initial dye concentration- 50 mg/L, sorbent dose- 0.1 g, agitation speed-150 rpm.

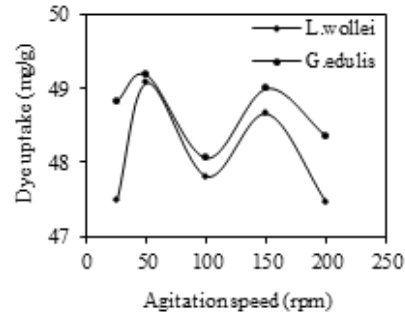


Fig. 4. Effect of shaking speed on sorption of BV 14 by *L.wollei* and *G.edulis* biomass. Contact time- 90 min, pH- 10, initial dye concentration- 50 mg/L, sorbent dose- 0.1 g, Temperature - 40°C.

The significance of sorbent particle size (<75 μm , 75-150 μm , 150-300 μm , 300-600 μm , >600 μm) on sorption of BV 14 is shown in Fig. 5. The dyes adsorbed increased as the sorbent particle size decreased. The sorption capacity of BV14 decreased from 97.1 to 94.1 mg/g for *L.wollei* and 82.5 to 78.1 mg/g for *G.edulis* as the particle sizes of <75 μm to >600 μm . The increase in dye uptake depends on the vast external surface area of small particles. The similar trend of adsorbent size effect was also reported for the adsorption of Methylene Blue onto Jordanian diatomite [28].

The influence of contact time (Fig. 6) was studied at 40°C while a sorbent dose of 0.10 g, a solution volume of 100 ml and an agitation speed of 50 rpm for a range of dye concentration. The rate of dye uptake was rapid at initial stage and equilibrium point has been reached within 90 min. This may be due to the fact that at the beginning of the sorption process all the reaction sites are vacant and hence the extent of removal is high. After a rapid initial uptake, there was a transitional phase in which the rate of uptake was slow with uptake reaching almost a constant value. Consequently, the adsorption of dyes was carried out in two distinct stages, a relatively rapid one followed by a slower one [29]. A similar result of the contact time effect was also reported for the adsorption of Basic violet 14 from aqueous solution on bentonite [30].

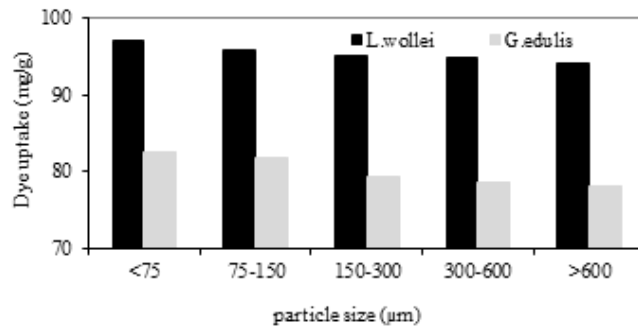
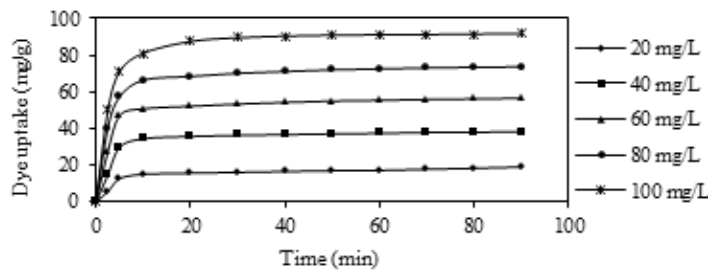
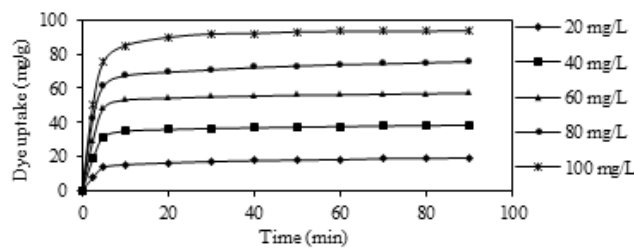


Fig. 5. Effect of particle size on sorption of BV 14 by *L.wollei* and *G.edulis* biomass. Contact time- 90 min, pH- 10, initial dye concentration- 50 mg/L, sorbent dose- 0.1 g, Temp- 40°C, agitation speed- 50 rpm.

The effect of initial dye concentration on the adsorption of BV 14 onto *L.wollei* and *G.edulis* biomass was deliberated by agitating 100 ml of dye solutions with concentrations of 20, 40, 60, 80, and 100 mg/L though the pH, shaking time, amount of sorbent, and temperature were fixed at 10, 90 min, 0.10 g, and 40°C, respectively. It was observed that the amount of dye adsorbed increased with the increase of initial dye concentration. Increasing the initial dye concentration increases the mass gradient between the solution and the adsorbent, and therefore, the rate at which dye molecules pass from the bulk solution to the particle surface and the amount of transfer at equilibrium [31].



(a) *L.wollei*



(b) *G.edulis*

Fig. 6. Effect of contact time on sorption of BV 14. pH- 10, sorbent dose- 0.1 g, Temp- 40°C, agitation speed-50 rpm.

3.2. Isotherm studies

The Langmuir equation is used for homogeneous surfaces. It is noted from Table 1 that the monolayer adsorption capacity (i.e., $q_{max} = 1250$ mg/g) of *G.edulis* is significantly superior to that of *L.wollei* (i.e., $q_{max} = 333.33$ mg/g) on sorption of BV 14. The n value (lies in between 1 -10) predicted by Freundlich isotherm indicates favourable sorption of BV 14 on both sorbents.

The higher value of correlation coefficients (Table 1) of Dubinin – Radushkevich isotherm model implies that sorption of BV 14 follows chemisorption on both sorbents, which has been confirmed with pseudo-second order equation and elovich model later.

The Temkin model yields better fit than other models, as reflected by correlation coefficients (R^2) of 0.980 and 0.991 for sorption onto *L.wollei* and *G.edulis*, respectively which has been confirmed with error function later.

Table 1. Isotherm constants for BV 14 sorption

Sorbents	Isotherm constants		
Langmuir	q_{max} (mg/g)	K_L (L/mg)	R^2
<i>L.wollei</i>	333.33	0.06	0.958
<i>G.edulis</i>	1250.0	0.016	0.975
Freundlich	K_F (mg/g)	n	R^2
<i>L.wollei</i>	20.79	1.385	0.951
<i>G.edulis</i>	21.28	1.164	0.972
Dubinin Radushkevich	q_s (mg/g)	k_{ad}	R^2
<i>L.wollei</i>	80.64	5.0×10^{-7}	0.965
<i>G.edulis</i>	86.49	5.0×10^{-7}	0.966
Temkin	A_t (L/mg)	B_t	R^2
<i>L.wollei</i>	1.657	78.07	0.980
<i>G.edulis</i>	1.557	65.0	0.991

3.3. Error functions

The values of error functions for all isotherm equations are listed in Table 2. By comparing the results of the values of the error functions, Temkin equation fitted well with sorption of BV 14 on to both sorbents.

Table 2. Error analysis of isotherm models for BV 14 sorption

Sorbents	ERRSQ/ SSE	HYBRID	MPSD	ARE	EABS/ SAE
Langmuir					
<i>L.wollei</i>	638.475	-13.790	20.923	14.43	45.517
<i>G.edulis</i>	393.24	-4.944	14.799	9.64	31.587
Freundlich					
<i>L.wollei</i>	109.739	-0.885	15.67	10.62	22.419
<i>G.edulis</i>	100.767	-0.316	12.14	8.20	19.071
Dubinin Radushkevich					
<i>L.wollei</i>	311.784	-4.4395	14.094	9.10	28.913
<i>G.edulis</i>	256.204	1.008	13.212	9.11	26.759
Temkin					
<i>L.wollei</i>	60.251	-2.161	7.194	5.53	15.529
<i>G.edulis</i>	24.91	-0.117	4.91	3.31	9.06

3.4. Sorption kinetics

The kinetic model parameters for sorption of BV 14 by *L.wollei* and *G.edulis* were presented in Tables 3 and 4 respectively. The correlation coefficients of pseudo first order kinetic model were low for both adsorbents. Also from the calculated values of q_e , it is observed that the sorption behaviour of both sorbents does not obey with the pseudo-first order kinetic model.

The higher correlation coefficient values and nearer theoretical values of q_e implies that sorption of BV 14 onto both sorbents pursue the pseudo-second order kinetic model *i.e.*, chemisorptions. The rate constant of adsorption was found to decrease with increasing the initial concentration.

In the first stage, the adsorption of dye takes place on the surface of both sorbents and is a rapid uptake stage. The values of k_{id1} and k_{id2} increased with increase in concentration. The increases of dye concentration result in increase of the driving force, which will increase the diffusion rate of the dye molecules. The dye uptake process was found to be controlled by intraparticle diffusion at second stages [32]. In the third stage, nearly the entire dynamic sites of the adsorbent were occupied by dye molecules and attain equilibrium. Intercept values (Table 4) give an idea about the thickness of the boundary layer, *i.e.*, the larger the intercept, the greater is the boundary layer effect [29]. The similar phenomenon was found on the adsorption of basic dyes from aqueous solution by various adsorbents [33].

Table 3. Kinetic model parameters for BV 14 sorption onto *L.wollei*.

Constants/ R^2	Initial dye concentration (mg/L)				
	20	40	60	80	100
q_e (mg/g) exp	18.90	38.21	56.45	73.66	91.85
Pseudo first-order model					
q_e (mg/g) cal	6.90	13.68	20.18	27.67	34.99
k_1 (min^{-1})	0.0483	0.0501	0.0529	0.0575	0.0575
R^2	0.920	0.909	0.915	0.931	0.934
pseudo second-order model					
q_e (mg/g) cal	19.23	40.00	58.82	76.92	100.00
k_2 (g/mg/min)	0.034	0.016	0.012	8.89 $\times 10^{-3}$	6.25 $\times 10^{-3}$
R^2	0.999	0.999	0.999	0.999	0.999
Intraparticle diffusion model					
k_{id1} (mg/g $\text{min}^{1/2}$)	5.29	10.93	16.68	21.37	26.61
I_1	1.528	2.361	3.249	3.701	4.054
R^2	0.917	0.946	0.939	0.948	0.964
k_{id2} (mg/g $\text{min}^{1/2}$)	0.390	0.682	0.985	1.353	1.402
I_2	15.41	32.08	47.61	61.77	79.94
R^2	0.925	0.915	0.967	0.912	0.775
Elovich model parameters at initial stage					
a (mg/g/min)	83.17	62.68	74.59	81.12	121.15
b (g/mg)	0.346	0.129	0.078	0.057	0.051
R^2	0.982	0.964	0.875	0.899	0.947

The Elovich rate equation is commonly used to describe the sorption behaviour with a rapid equilibrium rate in the early period, while it slows down the equilibrium at later periods of the sorption process. Along with increasing initial concentrations, the value of b decreases due to the less available surface (Table 4). Furthermore, the value of ' a ' should increase with initial concentrations because of the higher driving force. Therefore, the Elovich rate equation may not be suitable to describe the kinetics of BV 14 adsorbed onto both *L.wollei* and *G.edulis*.

Table 4. Kinetic model parameters for BV 14 sorption onto *G.edulis*.

Constants/ R^2	Initial dye concentration (mg/L)				
	20	40	60	80	100
q_e (mg/g) exp	18.99	38.31	57.09	75.65	93.85
Pseudo first-order model					
q_e (mg/g) cal	10.50	12.97	16.56	25.88	28.44
k_1 (min^{-1})	0.048	0.051	0.053	0.046	0.046
R^2	0.928	0.881	0.858	0.887	0.903
pseudo second-order model					
q_e (mg/g) cal	19.61	40.00	58.82	76.92	100.00
k_2 (g/mg/min)	0.0168	9.058×10^{-3}	0.0145	8.89×10^{-3}	9.09×10^{-3}
R^2	0.998	0.998	0.999	0.999	0.999
Intraparticle diffusion model					
k_{id1} (mg/g $\text{min}^{1/2}$)	5.03	11.58	17.68	22.31	28.10
I_1	0.235	0.955	1.846	3.789	3.791
R^2	0.960	0.960	0.957	0.952	0.963
k_{id2} (mg/g $\text{min}^{1/2}$)	0.616	0.545	0.623	1.294	1.169
I_2	13.38	33.27	51.33	63.65	83.95
R^2	0.982	0.989	0.985	0.991	0.799
Elovich model parameters at initial stage					
a (mg/g/min)	9.81	26.23	44.03	83.17	83.76
b (g/mg)	0.183	0.085	0.059	0.055	0.040
R^2	0.900	0.899	0.892	0.916	0.936

3.5. Sorbent characterization

Scanning electron microscopy images (magnification of X500, X1000, X5000) of adsorbents *L.wollei* and *G.edulis* was taken before and after dye adsorption. The

SEM images (Fig. 7) clearly show the possibility of dye molecules to be trapped and adsorbed into pores of sorbent.

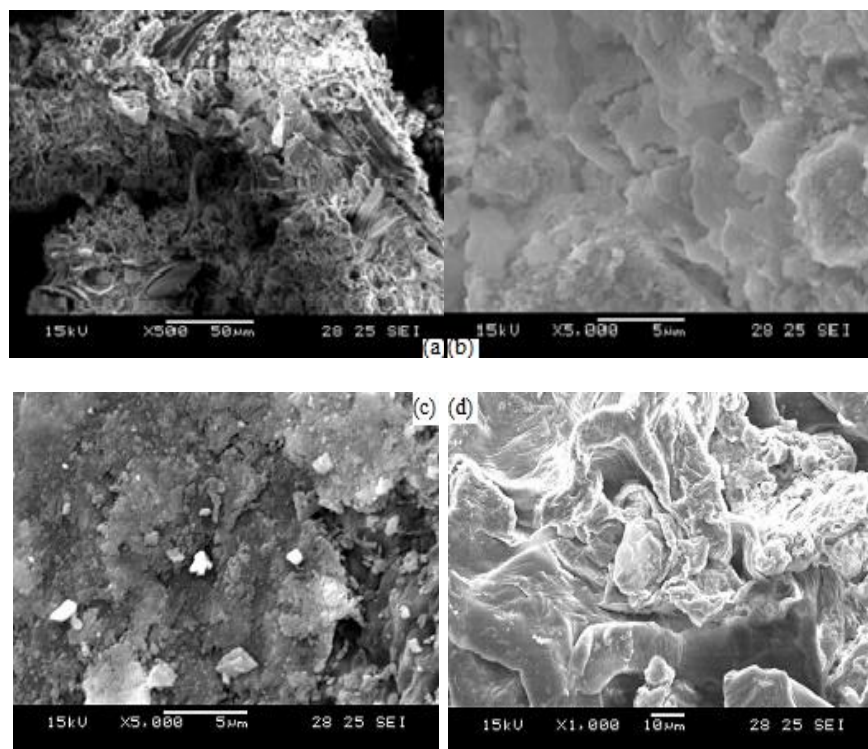


Fig. 7. SEM images of sorbents.

- (a) *L.wollei* before sorption process, (b) *L.wollei* adsorbed with BV 14,
 (c) *G.edulis* before sorption process, (d) *G.edulis* adsorbed with BV 14.

FTIR analysis of dye treated *L.wollei* exhibited highest peak at 3410.24 cm^{-1} for O-H and H bond stretching of alcohols and phenols. In addition all other peaks at 2922.74 cm^{-1} , 1641.46 cm^{-1} , 1428.54 cm^{-1} and 1035.61 cm^{-1} were elevated for C-H stretching of alkanes, N-H bending of 1° amines, CH_2 bending vibration $\text{CH}_2\text{-CO-}$ presence of carbonyl compounds, C-O stretch of carboxylic acids, esters and ethers respectively (Fig. 8(a)). In Fig. 8(b), Peak in the wave number of $1500\text{ cm}^{-1}\text{-}500\text{ cm}^{-1}$ indicated the vibrational modes that are specific to the type of polysaccharides and glycosidic linkages. Several peaks were obtained in this region. Peaks in these ranges denoted the presence of aldehyde functional groups which are actively involved in sorption. Amide I bands are (1639.32 cm^{-1}) due to C=O stretching vibrations of peptide bond provide insight into the protein secondary structure.

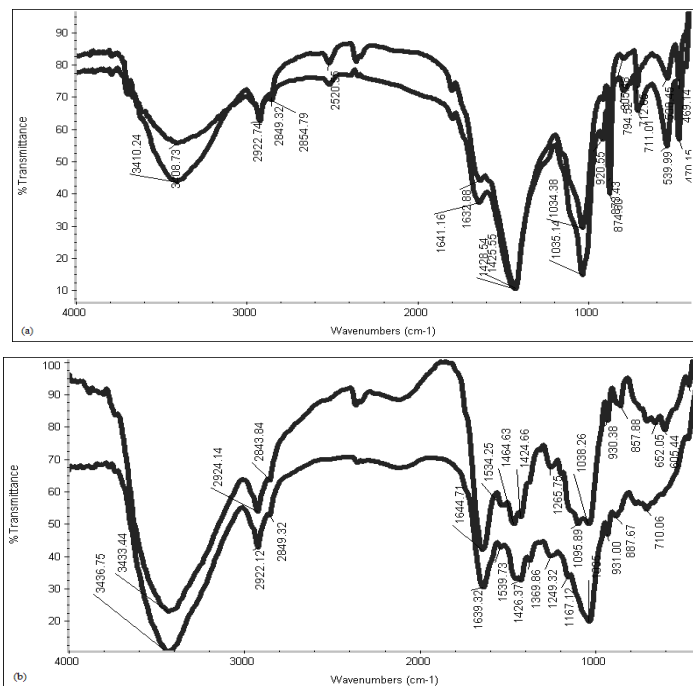


Fig. 8. FTIR spectra of sorbents before and after sorption of BV 14
(a) *L.wollei*, (b) *G.edulis*

4. Conclusions

The effectiveness of both brown seaweed (*Gracilaria edulis*) and fresh water algae (*Lyngbya wollei*) in sorption of basic violet 14 from aqueous solution was explored and compared. The dye uptake rate was rapid and attains equilibrium within 90 min at optimum temperature 40°C. Among all isotherm data obtained, the Temkin model yields a better fit than other models. The maximum adsorption capacity determined by Langmuir at optimum pH (pH 10), for *Gracilaria edulis* (1250.0 mg/g) was four times higher than *Lyngbya wollei* (333.33 mg/g). Error function provides the best parameters for the Temkin isotherm equation for this system. The adsorption kinetics of BV 14 can be well described by the pseudo-second-order model equation. The intraparticle diffusion rate constant was found to decrease with increasing the initial concentration. The SEM and FTIR images verified the sorption of BV 14 on both adsorbents.

References

1. Chen, A.H.; and Chen, S.M. (2009). Biosorption of azo dyes from aqueous solution by glutaraldehyde-crosslinked chitosans. *Journal of Hazardous Materials*, 172, 1111-1121.
2. Fu, Y.; and Vijayaraghavan, T. (2001). Fungal decolorization of dye wastewater: a review. *Bioresource Technology*, 79, 251-262.
3. Daneshvar, N.; Ayazloo, M.; Khataee, A.R.; and Pourhassan, M. (2007). Biological decolorization of dye solution containing Malachite Green by microalgae *Cosmarium sp.* *Bioresource Technology*, 98, 1176-1182.

4. Bhatnagar, A.; and Minocha, A.K. (2006). Conventional and non-conventional adsorbents for removal of pollutants from water- A review. *Indian journal of chemical technology*, 13, 203-217.
5. Chen, A.H.; and Huang, Y.Y. (2010). Adsorption of Remazol Black 5 from aqueous solution by the template crosslinked-chitosans. *Journal of Hazardous Materials*, 177(1-3), 668-675.
6. Bhatnagar, A.; Vilar, V.J.P.; Botelho, C.M.S.; and Boaventura, R.A.R. (2010). Coconut- based biosorbents for water treatment - A review of the recent literature. *Advances in Colloid and Interface Science*, 160, 1-15.
7. Rajeshkannan, R.; Rajasimman, M.; and Rajamohan, N. (2010). Optimization, equilibrium and kinetics studies on sorption of Acid Blue 9 using brown marine algae *Turbinaria conoides*. *Biodegradation*, 21, 713-727.
8. Langmuir, I. (1916). The constitution and fundamental properties of solids and liquids. *Journal of American Chemical Society*, 38(11), 2221-2295.
9. Freundlich, H. M. F. (1906). Over the adsorption in solution. *The Journal of Physical chemistry*, 57, 385-470.
10. Dubinin, M.M.; and Radushkevich, L.V. (1947). The equation of the characteristic curve of activated charcoal. *The Academy of Sciences-Physical Chemistry Section*, 55, 331-337.
11. Temkin, M.I.; and Pyzhev, V. (1940). Kinetics of ammonia synthesis on promoted iron catalyst. *Acta Physiochim, USSR*, 12, 327-356.
12. Foo, K.Y.; and Hameed, B.H. (2010). Insights into the modeling of adsorption isotherm systems. *Chemical Engineering Journal*, 156, 2-10.
13. Lagergren, S. (1898). About the theory of so-called adsorption of soluble substances. *Kungliga Svenska Vetenskapsakademiens Handlingar Band*, 24(4), 1-39.
14. Ho, Y.S.; and McKay, G. (1998). Sorption of dye from aqueous solution by peat. *Chemical Engineering journal*, 70, 115-124.
15. Weber, W.J.; and Morris, J.C. (1963). Kinetics of adsorption on carbon from solution. *Journal of Sanitary Engineering Division ASCE*, 89, 31-59.
16. Ho, Y.S.; and McKay, G. (1998). A Comparison of chemisorption kinetic models applied to pollutant removal on various sorbents. *Process Safety and Environmental Protection*, 76, 332-340.
17. Sparks, D.L.; and Jardine, P.M. (1984). Comparison of kinetic equation to describe potassium calcium exchange in pure and in mixed systems. *Soil Science*, 138 (2), 115-122.
18. Shah, J.; Jan, M.R., Haq, A.; and Khan, Y. (2013). Removal of Rhodamine B from aqueous solutions and wastewater by walnut shells: kinetics, equilibrium and thermodynamics studies. *Frontiers of Chemical Science and Engineering*, 7(4), 428-436.
19. Li, L.; Liu, S.; and Zhu, T. (2010). Application of activated carbon derived from scrap tires for adsorption of Rhodamine B. *Journal of Environmental Sciences*, 22(8), 1273-1280.
20. He, Y.; Gao, J.F.; Feng, F.Q.; Liu, C.; Peng, Y.Z.; and Wang, S.Y. (2012). The comparative study on the rapid decolorization of azo, anthraquinone and

- triphenylmethane dyes by zero-valent iron. *Chemical Engineering Journal*, 179, 8-18.
21. Shi, Q.; Zhang, J.; Zhang, C.; Nei, W.; Zhang, B.; and Zhang, H. (2010). Adsorption of Basic violet 14 in aqueous solutions using KMnO₄- modified activated carbon. *Journal of Colloid and Interface Science*, 343, 188-193.
 22. Wu, X.; Hui, K.N.; Hui, K.S.; Lee, S.K.; Zhou, W.; Chen, R.; Hwang, D.H.; Cho, Y.R.; and Son, Y.G. (2012). Adsorption of basic yellow 87 from aqueous solution onto two different mesoporous adsorbents. *Chemical Engineering Journal*, 180, 91-98.
 23. Ofomaja, A.E. (2007). Sorption dynamics and isotherm studies of methylene blue uptake on to palm kernel fibre. *Chemical Engineering Journal*, 126, 35-43.
 24. Tsai, W.T.; Chang, Y.M.; Lai, C.W.; and Lo, C.C. (2005). Adsorption of ethyl violet dye in aqueous solution by regenerated spent bleaching earth. *Journal of Colloid and Interface Science*, 289(2), 333-338.
 25. Argun, M.E.; Dursun, S.; Ozdemir, C.; and Karatas, M. (2007). Heavy metal adsorption by modified oak sawdust: Thermodynamics and kinetics. *Journal of Hazardous Materials*, 141, 77-85.
 26. Latif, M.M.A.; Ibrahim, A.M.; and Kady, M.F. (2010). Adsorption Equilibrium, kinetics and thermodynamics of methylene blue from aqueous solutions using biopolymer oak sawdust composite. *Journal of American Science*, 6(6), 267-283.
 27. Gurses, A.; Dogar, C.; Yalcin, M; Acikyildiz, M.; Bayrak, R.; and Karaca, S. (2006). The adsorption kinetics of the cationic dye, methylene blue, onto clay. *Journal of Hazardous Materials*, B131, 217-228.
 28. Al-Ghouti, M.A.; Khraisheh, M.A.M.; Ahmad, M.N.M.; and Allen, S. (2009). Adsorption behaviour of methylene blue onto Jordanian diatomite: A kinetic study. *Journal of Hazardous Materials*, 165, 589-598.
 29. Bayramoglu, G.; Altintas, B.M.; and Arica, Y. (2009). Adsorption kinetics and thermodynamic parameters of cationic dyes from aqueous solutions by using a new strong cation-exchange resin. *Chemical Engineering Journal*, 152, 339-346.
 30. Jiang, Y.X.; Xu, H.J.; Liang, D.W.; and Tong, Z.F. (2008). Adsorption of Basic Violet 14 from aqueous solution on bentonite. *C.R. Chimie*, 11, 125-129.
 31. Reddy, D.H.K.; Lee, S.M.; and Seshaiiah, K. (2012). Removal of Cd (II) and Cu(II) from aqueous solution by agro biomass: Equilibrium, kinetic and thermodynamic studies. *Environmental Engineering Research*, 17(3), 125-132.
 32. Patil, S.; Deshmukh, V.; Renukdas, S.; and Patel, N. (2011). Kinetics of adsorption of crystal violet from aqueous solutions using different natural materials. *International Journal of Environmental Sciences*, 6, 1116-1134.
 33. Shiau, C.Y.; and Pan, C.C. (2004). Adsorption of basic dyes from aqueous solution by various adsorbents. *Separation science and technology*, 39(8), 1733-1750.